

# A Gaskinetic Scheme for Nonequilibrium Planar Shock Simulations

Chunpei Cai\* Khaleel R.A. Khasavneh†

*New Mexico State University, Las Cruces, New Mexico 88003*

Shuchi Yang‡ Danny D. Liu§

*ZONA Technology Inc., Scottsdale, Arizona 85258*

This paper reports some preliminary progress in developing a gaskinetic Computational Fluid Dynamic scheme, based on the Bhatnagar-Gross-Krook(BGK) model, to simulate a planar nitrogen shock wave with thermochemical nonequilibrium effects. The scheme is applicable for gas flows with thermal nonequilibrium effects, i.e., translational, rotational and vibrational energy relaxations, and with dissociation and recombination chemical reactions. We determine the post-shock boundary conditions with a consideration of detailed equilibrium satisfying general Rankine-Hugoniot relations. Different from those past studies which are based on the Boltzmann-like equation and split the collision term into elastic and chemical collision terms, here we consider the chemical reactions by treating them as source terms. This treatment renders us a much simpler scheme than gaskinetic schemes relying on detailed collisions. The merits of this scheme include a relatively faster computation speed than particle simulation methods and gaskinetic schemes based on the full Boltzmann equation. The gaskinetic BGK simulation results are validated with those obtained with the direct simulation Monte Carlo (DSMC) method.

## Nomenclature

$f$	=velocity distribution function with multiple temperatures
$g$	=equilibrium velocity distribution function
$m$	=atomic mass
$n$	=normal direction to a local cell edge
$k$	=Boltzmann constant
$p$	=pressure
$u, v, w$	=particle velocity
$E$	=energy
$F$	=macroscopic flux across a cell face
$K$	=degree of freedom
$R$	=gas constant
$S$	=source term vector
$T$	=macroscopic temperature
$U$	=macroscopic mean velocity components
$W$	=macroscopic property variables
$Q$	=participation function

---

\*Assistant Professor, Department of Mechanical and Aerospace Engineering. Previously worked as a CFD Specialist at ZONA Technology Inc. AIAA Senior Member.

†Ph.D. graduate student, Department of Mechanical and Aerospace Engineering.

‡CFD Specialist, 9489 E. Ironwood Square Drive, AIAA Senior Member.

§Company President. Professor Emeritus Arizona State University, 9489 E. Ironwood Square Drive, AIAA Fellow.

$Z_r$	=specific rotational energy relaxation number
$Z_v$	=specific vibrational energy relaxation number
$\alpha$	=degree of dissociation
$\lambda$	= $1/(2RT)$
$\gamma$	=specific heat ratio, $=C_p/C_v$
$\rho_d$	=characteristic density for dissociation
$\tau$	=characteristic relaxation time
$\mu$	=viscosity
$\rho$	=density
$\xi$	=internal particle velocity, $\xi^2 = \xi_t^2 + \xi_v^2 + \xi_r^2$
$\Theta_v$	=characteristic vibrational temperature for nitrogen molecule
$\Theta_d$	=characteristic dissociation temperature for nitrogen molecule
$^{eq}$	=equilibrium state
$t, r, v$	=properties associated with translational, rotational and vibrational temperatures
$\infty$	=freestream flow properties
$BGK$	=Bhatnagar-Gross-Krook model
$CFD$	=Computational Fluid Dynamics
$Kn$	=Knudsen number
$MHD$	=Magnetohydrodynamic
$Pr$	=Prandtl number

## I. Introduction

Hypersonic flows are characterized by shock waves with several kinds of nonequilibrium effects, such as thermal nonequilibrium, chemical nonequilibrium, and ionization/MagnatoHydroDynamics (MHD) effects. As such, to accurately capture the inner structure of shock waves with real gas effects, has been an important research topic for decades. In the past years, much effort on experiments, numerical simulations and modeling has been reported. For example, the book by Zel'dovich<sup>1</sup> discussed inner structure of shock waves with details. Groppi *et al*<sup>2-4</sup> and Rossino *et al*<sup>5</sup> reported several studies of shock structures with four species, by neglecting all internal degree of freedom, but with careful microscopic modeling. In these papers, the collision terms for the Boltzmann-like equations are split into two parts, one for elastic collisions, and the other for chemical collisions. They also provide a detailed review of gaskinetic modeling work as well.

This paper aims to report our recent preliminary progress in developing a gaskinetic scheme<sup>6</sup> to simulate chemically reacting gas flows. This scheme is based on the Bhatnagar-Gross-Krook (BGK) model of the Boltzmann equation, and it is applied to simulate a planar nitrogen shock wave with thermal and chemical nonequilibrium effects. This scheme has many merits, for example, the flux computation is simple, unlike the classical Computational Fluid Dynamics (CFD) schemes which evaluate the inviscid/viscous, and equilibrium/nonequilibrium fluxes with several steps, this gaskinetic BGK scheme evaluates all fluxes with one step, hence it is much simpler with less numerical dissipation.<sup>6-8</sup> This gaskinetic scheme is also more suitable to simulate a wider range of rarefied gas flows with a pressure range from a few hundred of atmospheres to very low pressure,<sup>9</sup> because of its closer link to the kinetic Boltzmann equation.<sup>10</sup> As such, once properly developed for chemically reacting flows, this scheme is applicable used to simulate hypersonic flows around a reentry vehicle or a ballute, applicable to a much higher altitude. This merit may relieve the direct simulation Monte Carlo(DSMC)<sup>11</sup> method from the expensive computation burden at a low altitude.

This special gaskinetic BGK scheme is promising for hypersonic flow computations, and the work described in this paper is a natural extension of our past work.<sup>12</sup> Previously, we have successfully developed a gaskinetic CFD scheme for planar nitrogen shock wave computation with thermal nonequilibrium effects, and it successfully captures the thermal nonequilibrium effects across a planar shock wave. This paper aims to develop a new gaskinetic CFD scheme to simulate the inner structure of thermal-chemically nonequilibrium

planar shock waves with two species. More specifically we are interested to observe whether this new scheme can capture different kinds of relaxation processes.

This paper is organized as follows: Section II explains the detailed procedure to determine the downstream boundary conditions, which are critical for the shock wave simulations; Section III presents the key steps in the newly designed and implemented gaskinetic CFD scheme based on the BGK model, and treatment of chemical reactions; Section IV provides some validation results, computed with the newly developed gaskinetic scheme, and compared with the past result in the literature; Section V wraps up this paper with several conclusions.

## II. Downstream Boundary Conditions

To accurately perform a shock wave simulation with the DSMC and gaskinetic BGK methods, one key condition is to properly determine the post-shock equilibrium state as fixed boundary conditions. That is because the post-shock downstream shall utilize Dirichlet type rather than Neumann boundary conditions. However, traditional Rankine-Hugoniot relations are not applicable here because we consider inner degree of freedom and dissociation-recombination effects with non-constant specific heat ratio across the shock wave. Previously, we used a set of generalized Rankine-Hugoniot relations across a planar shock wave with a consideration of inner rotational and vibrational energies.<sup>12</sup> To determine the downstream equilibrium boundary conditions, there are several treatments<sup>13,14</sup> in the literature, here we develop one based on some relations in the book by Vincenti and Kruger.<sup>14</sup>

Take a long control volume, with one end at the pre-shock equilibrium state with pressure  $p_1$ , temperature  $T_1$ , number density  $n_1$ , density  $\rho_1$ ; the other end at the post shock equilibrium state as well, where all thermal and chemical relaxation processes have completed, and the degree of dissociation is denoted as  $\alpha$ ,<sup>14</sup> the pressure, density and temperature are denoted as  $p_2$ ,  $\rho_2$ , and  $T_2$ . Then, the mass, momentum, energy, equilibrium state dissociation equations, and equation of state are:<sup>1,14</sup>

$$\rho_1 u_1 = \rho_2 u_2 \quad (1)$$

$$p_1 + \rho_1 u_1^2 = p_2 + \rho_2 u_2^2 = (1 + \alpha)\rho_2 R_{N_2} T_2 + \rho_2 u_2^2 \quad (2)$$

$$\frac{\gamma_1}{\gamma_1 - 1} R_{N_2} T_1 + \frac{u_1^2}{2} = \frac{u_2^2}{2} + \frac{P_2}{\rho_2} + \frac{3}{2} R_N T_2 \alpha + (1 - \alpha) \left[ \frac{5}{2} R_{N_2} T_2 + \frac{R\theta_v}{\exp(\theta_v/T) - 1} \right] + \alpha \Theta_d R_{N_2} \quad (3)$$

$$\frac{\alpha^2}{1 - \alpha} = \frac{\rho_d(T_2)}{\rho_2} \exp(-\theta_d/T_2) \quad (4)$$

$$p_2 = (1 + \alpha)\rho_2 R_{N_2} T_2 \quad (5)$$

where  $\rho_d$  is the characteristic density for dissociation,<sup>14</sup>  $\rho_d = m_N (\frac{\pi m_N k}{h^2})^{3/2} \Theta_r \sqrt{T_2} [1 - \exp(-\Theta_v/T_2)] \frac{(Q_{el}^N)^2}{Q_{el}^{NN}}$ , and  $Q_{el}^N = 4$ ,  $Q_{el}^{NN} = 1$ .<sup>14</sup> When  $\alpha = 0$  and the vibrational energy is frozen then the above equations compatibly revert to relations leading to the classical Rankine-Hugoniot relations. It should be pointed out that the above relations are only approximate, for example, electron energy is neglected in Eqn.(3).

A special iteration process is adopted to solve the above five equations. The free stream conditions are, nitrogen gas,  $\rho_\infty = 1.741315 \times 10^{-3} \text{ kg/m}^3$ ,  $T_\infty = 226.649 \text{ K}$ , and a properly given Mach number.

Figure 1 shows the post-shock equilibrium state density and pressure profiles with and without considerations of dissociation effects. The pressure profiles do not have much difference, no matter the dissociation effects are considered or not. This trend is consistent with the assumption used by Zel'dovich<sup>1</sup> to estimate the dissociation distance. One density profile is the result by considering vibrational energy effect but without dissociation effect, and it shows a relatively flat hypersonic asymptote value, but the value is  $(\gamma_2 + 1)/(\gamma_2 - 1) < 6$ . This is because  $\gamma_2$  is different from 1.4 with a consideration of variable and vibrational energy and chemical reactions. Another density profile has increasing density values as the upstream Mach number increases, with stronger dissociations.

Figure 2 shows the dissociation rate and post shock temperature profiles vs. the free stream Mach number. With stronger free stream Mach number, the degree of dissociation continues to increase because of the higher post-shock temperature. The post-shock temperature without dissociation-recombination effects actually increase fairly fast; while the other with a consideration of dissociations changes very slowly. Physically this is correct, with stronger shock wave, the post-shock wave region has higher temperature, which favors more chemical dissociations. Most of the energy is spent on breaking the bonds between atoms, instead of increasing the thermal temperature.

### III. A Gaskinetic CFD Scheme for Hypersonic Gas Flow Computations

#### A. Descriptions for the Gaskinetic CFD Scheme

We developed one gaskinetic CFD scheme to simulate gas flows dissociation-recombination reactions, and this section briefly presents the key steps for this scheme.

The Boltzmann equation expresses the behavior of a many particle kinetic system in terms of the evolution equation for a single particle gas distribution function. The right-hand side of the Boltzmann equation is mainly two body collisions that are valid for a large range of pressure, from several hundreds of atmospheres to free-molecular flow.<sup>9</sup> To simplify the Boltzmann equation, the one-dimensional BGK models for  $N_2$  and  $N$  are used here:

$$\frac{\partial f_s}{\partial t} + u \frac{\partial f_s}{\partial x} = \frac{g_s - f_s}{\tau_s} \quad (6)$$

where subscripts  $s = 1, 2$  represent species for  $N_2$  and  $N$ ,  $f_s$  is the normalized number density distribution of molecules at position  $x$  with a particle velocity  $u$  at time  $t$ ,  $\tau_s = \mu_s/p_s$  is the characteristic relaxation time,  $\mu_s$  is viscosity computable by Sutherlands law or by a power law, and  $g_s$  are the equilibrium states with the following specific Maxwellian expressions:

$$g_1 = \rho_1 \left(\frac{\lambda_{x1}}{\pi}\right)^{3/2} \exp(-\lambda_{x1}(u - U)^2 - \lambda_{x1}\xi_t^2) \left(\frac{\lambda_r}{\pi}\right)^{K_r/2} \exp(-\lambda_r\xi_r^2) \left(\frac{\lambda_v}{\pi}\right)^{K_v/2} \exp(-\lambda_v\xi_v^2) \quad (7)$$

$$g_2 = \rho_2 \left(\frac{\lambda_{x2}}{\pi}\right)^{3/2} \exp(-\lambda_{x2}(u - U)^2 - \lambda_{x2}\xi_t^2) \quad (8)$$

where  $\rho$  is the density,  $U$  the macroscopic fluid velocity along the flow direction,  $\lambda = m/(2kT)$ ,  $m$  the molecular mass,  $k$  the Boltzmann constant, and  $T$  a specific temperature. For an equilibrium flow, an internal variable  $\xi$  accounts for the translational, rotational and vibrational modes for nitrogen gas and has an expression of  $\xi^2 = \xi_t^2 + \xi_r^2 + \xi_v^2$  in which  $\xi_t, \xi_r, \xi_v$  are translational, rotational, vibrational phase velocities respectively, and  $K_r, K_v$  are the degrees of freedom for rotational and vibrational energy respectively. For nitrogen atoms, there is no rotational and vibrational energy, and the degree of freedom for inner translational energy is 2. Here we assume three different temperatures, translational, rotational and vibrational temperature for nitrogen gas; while for nitrogen atom, the equilibrium state is only characterized by one translational temperature. To further simplify the work, here we assume the nitrogen atom has the same translational temperature and average macroscopic average velocity as the nitrogen gas. It should be pointed out that this aims to reduce the number of equations; with less assumptions and more sophisticated modeling work, different translational temperatures and bulk velocity can be assumed for nitrogen gas and atom. However, it inevitably increases the numbers of equations and hence complexity.

Due to the inner degrees of energy, the specific heat ratio for nitrogen molecules is a complex function, and it can be defined as:

$$\gamma_1 = \frac{3 + K_r + K_v + 2}{3 + K_r + K_v} \quad (9)$$

which is a function of rotational and vibrational energy. For nitrogen atom, the specific heat ratio  $\gamma_2 = 5/3$ .

The mass  $\rho_1$  and  $\rho_2$ , total momentum  $\rho U$ , total energy  $\rho E$ , rotational energy  $\rho_1 \epsilon_r$ , and vibrational energy  $\rho_1 \epsilon_v$ , has the following relations with the gas distribution functions  $f_1$  and  $f_2$ :

$$W = (\rho_1, \rho_2, \rho U, \rho E, \rho_1 \epsilon_r, \rho_1 \epsilon_v)^T = \int \Psi_1 f_1 du d\xi_t d\xi_r d\xi_v + \int \Psi_2 f_2 du d\xi_t \quad (10)$$

where  $\rho = \rho_1 + \rho_2$  and  $\Psi_1, \Psi_2$  are defined as follows:

$$\Psi_1 = (1, 0, u, \frac{1}{2}(u^2 + \xi_t^2 + \xi_r^2 + \xi_v^2), \frac{1}{2}\xi_r^2, \frac{1}{2}\xi_v^2), \Psi_2 = (0, 1, u, \frac{1}{2}(u^2 + \xi_t^2), 0, 0). \quad (11)$$

Based on the preceding BGK models, the Navier-Stokes equations can be derived with the Chapman-Enskog expansion with the first order expression only,<sup>15</sup> for these two species:

$$f_s = g_s - \tau_s (\partial g_s / \partial t + u \partial g_s / \partial x) \quad (12)$$

where  $s = 1, 2$  are for nitrogen molecules and atoms, correspondingly. To provide the gradients for  $g_s$ , the density,  $\rho$ , average velocity,  $U$ , and  $\lambda$  are assumed to be functions of both time and space. The process to

compute the slopes in the equilibrium distributions in Eqn.(12) is quite complex but crucial for the gaskinetic CFD scheme, we briefly describe it as follows.

The equilibrium state of nitrogen gas is described by Eqn.(7), since

$$(\rho_1, \rho_1 U, \rho_1 E, \rho_1 E_t, \rho_1 E_r, \rho_1 E_v)^T = \int g_1 \Psi'_1 dud\xi_t d\xi_r d\xi_v \quad (13)$$

where  $\rho_1 E$ ,  $\rho_1 E_t$ ,  $\rho_1 E_r$  and  $\rho_1 E_v$  are the total, translational, rotational and vibration energy for nitrogen gas, correspondingly, and  $\Psi' = \{1, u, \frac{1}{2}(u^2 + \xi_t^2 + \xi_r^2 + \xi_v^2), \frac{1}{2}\xi_t^2, \frac{1}{2}\xi_r^2, \frac{1}{2}\xi_v^2\}$ .

By the Taylor expansion, we assume:

$$\frac{\partial g_1}{\partial x} = (a_1 + a_2 u + a_3 u^2 + a_4 \xi_t^2 + a_5 \xi_r^2 + a_6 \xi_v^2)g \quad (14)$$

and relations among macroscopic property gradients and velocity distribution function are:

$$\frac{\partial}{\partial x}(\rho_1, \rho_1 U, \rho_1 E, \rho_1 E_t, \rho_1 E_r, \rho_1 E_v)^T = \int \frac{\partial g_1}{\partial x} \Psi'_1 dud\xi_t d\xi_r d\xi_v. \quad (15)$$

The above equations have the following solutions:<sup>12</sup>

$$a_6 = \frac{4\lambda_v^2}{K_v} \frac{\partial(\rho_1 E_v)}{\rho_1 \partial x} - \frac{\partial \rho_1}{\rho_1 \partial x} \lambda_v, a_5 = \frac{4\lambda_r^2}{K_r} \frac{\partial(\rho_1 E_r)}{\rho_1 \partial x} - \frac{\partial \rho_1}{\rho_1 \partial x} \lambda_r, a_4 = \frac{4\lambda_t^2}{2} \frac{\partial(\rho_1 E_t)}{\rho_1 \partial x} - \frac{\partial \rho_1}{\rho_1 \partial x} \lambda_t$$

Then, define

$$A = \frac{\partial \rho_1}{\rho_1 \partial x} - \frac{K_v}{2\lambda_v} a_6 - \frac{K_r}{2\lambda_r} a_5 - \frac{1}{\lambda_t} a_4; B = \frac{\partial(\rho_1 U)}{\rho_1 \partial x} - \frac{\partial \rho_1}{\rho_1 \partial x} U$$

$$C = \frac{\partial(\rho_1 E)}{\rho_1 \partial x} - \frac{\partial(\rho_1 E_t)}{\rho_1 \partial x} - \frac{\partial(\rho_1 E_r)}{\rho_1 \partial x} - \frac{\partial(\rho_1 E_v)}{\rho_1 \partial x} - \frac{1}{4}(U^2 + \frac{1}{2\lambda_x})(\frac{2a_4}{\lambda_t} + \frac{K_r a_5}{\lambda_r} + \frac{K_v a_6}{\lambda_v}) - \frac{A}{2}(U^2 + \frac{1}{2\lambda_x})$$

we have the rest relations as:

$$a_3 = 4\lambda_x^2(C - BU), a_2 = 2\lambda_x(B - \frac{Ua_3}{\lambda_x}), a_1 = A - (U^2 + \frac{1}{2\lambda_x})a_3 - Ua_2 \quad (16)$$

The above procedure is to compute the spatial gradient for the nitrogen gas,  $\partial g_1 / \partial x$ . As for the temporal gradient  $\partial g_1 / \partial t$ , it is linked with the spatial gradient, and can be obtained from the later conveniently with compatible relations.<sup>6,16</sup> As for the nitrogen atom, the temporal and spatial gradients,  $\partial g_2 / \partial x$  and  $\partial g_2 / \partial t$ , are relatively simple to compute since only one translational temperature is involved.

An operator-splitting method is used to solve Eqn.(6). Here is the general solution of  $f_1$  for the nitrogen gas in the BGK model with the inclusion of the  $(g_1 - f_1) / \tau_s$  term of Eqn.(6) at a cell interface  $x_{j+1/2}$  and time  $t$ :<sup>9</sup>

$$f_1(x_{j+1/2}, t, u, \xi_t, \xi_r, \xi_v) = \frac{1}{\tau_1} \int_0^t g_1(x, t', u, \xi_t, \xi_r, \xi_v) \exp(-(t-t')/\tau_1) dt' + \exp(-t/\tau_1) f_{01}(x_{j+1/2} - ut) \quad (17)$$

where  $x = x_{j+1/2} - u(t - t')$  is the particle trajectory, and  $f_{01}$  is the initial gas distribution function at the beginning of each time step ( $t=0$ ). How to properly construct  $f_{01}$  was explained in one of Xu's paper.<sup>6</sup> The preceding solution essentially combines the particle movement and particle collision effects into one step, hence viscous and inviscid fluxes are computed in one procedure step as well. This is one of the most fundamental advantages for the gaskinetic CFD scheme based on the BGK model, over traditional CFD schemes based on the Navier-Stokes equations.

There are six equations to be solved, two mass conservation equations for the nitrogen gas and atom, respectively, one global momentum equation for  $N_2$  gas and  $N$  atom, three equations for energy: one for total energy of nitrogen gas and atom, and the other two for the rotational and vibrational energy equations of nitrogen gas. Five of the six equations, except the total momentum equation, have source terms, due to chemical reactions and energy relaxation processes. For convenience, we denote the source term as  $S = (s_1, s_2, 0, s_4, s_5, s_6)$ . The source term for the nitrogen gas mass equation,  $s_1$ , must be equal to  $-s_2$ , to maintain mass conservation, the destroying rate for nitrogen gas equals to the creation rate of nitrogen atom. There is no source term in the general momentum equation because we consider the momentum of

the nitrogen gas and atom together. There is a source term in the total energy equation, it is directly related with the nitrogen gas dissociation rate and the dissociation energy. The source terms for the rotational and vibrational energy have special formats that the corresponding rotational and vibrational temperatures relax to the averaged translational temperature. Detailed source term modeling work is summarized in the next subsection.

The relation between the fluxes and the gas distribution function  $f_s$  is

$$F = \int \Psi_1 u f_1 du d\xi_t d\xi_r d\xi_v + \int \Psi_2 u f_2 du d\xi_t \quad (18)$$

A finite volume method is used to solve the BGK model:<sup>7,8</sup>

$$W_j^{n+1} = W_j^n + \frac{1}{\Delta x} \int_0^{\delta t} [F_{j-1/2}(t) - F_{j+1/2}(t)] dt + S_j^n \delta t \quad (19)$$

where  $W_j^n$  is the cell-averaged mass, momentum, total energy, nitrogen gas rotational energy, and nitrogen gas vibrational energy, and  $F_{j+1/2}$  is the corresponding fluxes at a cell interface by integrating the velocity distribute functions with Eqn.(18). For the computations of the inner structures for a planar shock wave, the temperature profiles are the major concerns. Hence, a correct heat-flux relation is crucial for the computation. It is well known that the BGK model incorrectly provides a Prandtl number,  $Pr=1$ , after taking moments to obtain the corresponding Navier Stokes equations. Hence, the heat flux in the energy flux is not correct:

$$q_1 = \frac{1}{2} \int (u - U)[(u - U)^2 + \xi_t^2 + \xi_r^2 + \xi_v^2] f_1 du d\xi_t d\xi_r d\xi_v \quad (20)$$

$$q_2 = \frac{1}{2} \int (u - U)[(u - U)^2 + \xi_t^2] f_2 du d\xi_t \quad (21)$$

The simplest but most effective treatment is the Prandtl number fix,<sup>6</sup> which is used in this study as well:

$$F_{Es}^{new} = F_{Es} + \left(\frac{1}{Pr} - 1\right) q_s \quad (22)$$

where  $F_{Es}$ ,  $s=1, 2$  are the two terms in the energy fluxes described by Eqn.(18).

Another important issue is to determine the characteristic relaxation time step  $\tau_s$ . In this study, we adopt the following format to compute the parameter  $\tau_s$  for each cell at each time step, for nitrogen gas and atom respectively:<sup>6</sup>

$$\tau_s = \frac{\mu_s}{p_s} + \frac{|\rho_{sl}/\lambda_{sl} - \rho_{sr}/\lambda_{sr}|}{|\rho_{sl}/\lambda_{sl} + \rho_{sr}/\lambda_{sr}|} \Delta t \quad (23)$$

where subscripts  $l$  and  $r$  represent quantities at the left and right cell center and  $\Delta t$  is the Courant-Friedrichs-Lewy (CFL) time step. The second part corresponds to the numerical viscosity.<sup>6</sup>

## B. Chemical Reaction and Relaxation Term Modeling

Unavoidably, some modeling work is needed here for the five source terms mentioned in the previous subsection, and they create some uncertainties in the simulation results.

For the nitrogen gas inner rotational and vibrational energy, we adopted the following traditional models:

$$s_5 = \rho_2 R_{N_2} (T_r - T_{tr}) / (Z_r \tau_2), s_6 = \rho_2 R_{N_2} [T_v - e_v(T_{tr})] / (Z_v \tau_2), \quad (24)$$

where  $T_r, T_v$  and  $T_{tr}$  are internal rotational, vibrational and translational temperatures, respectively.  $Z_r$  and  $Z_v$  are the relaxation parameters for rotational and vibrational temperatures. In this scheme, we assume the rotational and vibrational temperature relax toward the equilibrium translational temperature, based on the fact that the internal rotational and vibrational energy is obtained via energy exchange with the translational energy. Further, we choose typical relaxation numbers,  $Z_r = 3$  and  $Z_v = 30$ . Of course, the introduction of these two numbers leads to some uncertainty in the simulation results. We must point it out that  $T_{tr}$  is the same translational temperature for nitrogen gas and atoms, hence this treatment considers collisions between molecule-molecule and molecule-atoms. However, this treatment is different from the equal partition of energy within all degrees of freedom in the DSMC method, hence some discrepancies are expected here.

As for chemical reactions, there are a few options on different levels available. Lian and Xu<sup>17</sup> previously developed a two-dimensional gaskinetic CFD scheme for chemically reacting denotation shock wave computation, where the viscosity is neglected while chemical reactions are included as source terms. On the bottom level, we have the Boltzmann-like equations which split the right hand side collision term into a combination of elastic and chemical collision terms.<sup>2,18,19</sup> Even though this treatment sounds accurate, however, some modeling is unavoidable which will sacrifice the accuracy. In addition, these treatment is very expensive for computation. In this study, one major goal is to achieve high computation efficiency, hence some simplification are favored. Hence, we treat the chemical collision effects as additional source terms in the BGK scheme. Within each time step, we use traditional chemical reaction formula as one additional sub-step. This treatment is akin to chemical reaction source terms in Navier-Stokes equation solvers, and due to the small computation step comparable to the characteristic relaxation time step, this treatment is more favored here due to its simplicity and computation efficiency.

The following simple chemical reactions are considered here:<sup>14</sup>



where  $M$  represents a third body, either a nitrogen molecule or a nitrogen atom. The dissociation rate coefficients were determined from the following rate data:<sup>20</sup>

$$\begin{aligned} k_{f1}(N_2 - N) &= 1.41 \times 10^{-4} T^{-3.5} \exp(-113200/T) \quad m^3/molecules/sec \\ k_{f2}(N_2 - N_2) &= 3.82 \times 10^{-1} T^{-3.5} \exp(-113200/T) \quad m^3/molecules/sec \end{aligned} \quad (26)$$

The equilibrium constant  $K_c(N_2)$  is taken from Vincenti and Kruger:<sup>14</sup>

$$K_c(N_2) = 1.084 \times 10^{31} \exp(-113200/T) \quad (27)$$

And the nitrogen atom production rate is:

$$d[N]/dt = 2 \left[ k_{f1}[N] + k_{f2}[N_2] \right] \left[ [N_2] - [N]^2/K_c \right] \quad (28)$$

The remaining source terms  $s_1, s_2, s_4$  in Eqn.(19) are:

$$s_2 = -s_1 = M_N d[N]/dt = 2M_N \left[ k_{f1}[N] + k_{f2}[N_2] \right] \left[ [N_2] - [N]^2/K_c \right] \quad (29)$$

$$s_4 = -M_N \frac{d[N]}{dt} \Theta_d R_{N_2} = -s_1 \Theta_d R_{N_2} \quad (30)$$

where  $M_N$  is the nitrogen atom molecular mass. The dissociation rate for nitrogen gas should be equal to the creation rate for nitrogen atoms. For the energy source term  $s_4$ , the nitrogen dissociation absorbs a certain amount of energy to break the bounds between nitrogen atoms inside a molecule, hence the source term is directly proportional to the nitrogen atom creation rate. The nitrogen gas internal rotational and vibrational energy relaxation source terms was mentioned as Eqn.(24).

These chemical reactions are treated as source terms, and the rationale behind this scheme is related to the Navier-Stokes solvers, which separate the chemical reaction flux term from the viscous and inviscid fluxes. Hence, the gaskinetic BGK solver here evaluate the inviscid and viscous flux in one term and treat this chemical reactions and rotational and vibrational energy relaxation as source terms as well.

This treatment for chemical reactions rates is consistent with the downstream and upstream equilibrium states, with the equilibrium temperature, the rate of dissociation and recombination between nitrogen molecules and nitrogen atom are balanced at the upstream and downstream. Hence there is no density change at these two equilibrium states, respectively, and stable boundary conditions are achieved.

## IV. Numerical Simulations

With a set of properly determined post shock boundary conditions, we can perform simulations with the developed scheme and compare the results with those obtained by DSMC simulations. In those simulations, nitrogen molecules dissociate and nitrogen atoms recombine through strong planar shock waves. The validation case is chosen from one experiment case by Kewley and Hornung.<sup>21</sup> The free stream conditions are, pure

nitrogen gas, static pressure  $p_\infty = 666.1$  Pa, density  $\rho_\infty = 7.48 \times 10^{-3}$  kg/m<sup>-3</sup>, and macroscopic average velocity  $U_\infty = 7310$  m/s. This case has been widely simulated in the past with DSMC simulations.<sup>13,22</sup>

Figure 3 shows the density ratio profiles across the shock wave. The solid line is computed with the gaskinetic BGK scheme, the dash-dotted line represents DSMC simulation results by Bird,<sup>13</sup> and the dash line represents another set of DSMC simulation results by Boyd,<sup>22</sup> and some experimental results measured by Kewley and Hornung<sup>21</sup> are also displayed with circular symbols. In general, the gaskinetic BGK scheme predicts a much steep density profile than DSMC simulation results. This is a well-known defect for gaskinetic schemes based on the BGK model, and in the future we are planning to adopt the  $\tau_*$  approach<sup>23</sup> to improve this problem. The  $\tau_*$  approach includes higher gradient terms in the characteristic relaxation time, and it is proved effective to improve simulation accuracy. Figure 4 shows the normalized density profile, nitrogen gas and atom percentage profiles across the shock wave. In front of the shock wave, the gas is pure nitrogen gas with low temperature, hence the nitrogen gas percentage is 100%, while across the strong shock wave, the temperature increases, and strong dissociations happen. Hence, the nitrogen gas percentage drops while nitrogen atom percentage increases. The chemically relaxation process is the slowest one across the shock wave. By comparison, translational relaxation completes the fastest, followed by the rotational energy relaxation next, and the vibrational energy relaxation. Figure 4 shows the density profile and mass percentage profiles are very smooth, and those properties converge to the downstream values very smoothly and naturally. There are no kinks at the downstream boundary, indicating our downstream boundary treatment is valid.

Figure 5 shows translational temperature profiles computed by the gaskinetic BGK and the DSMC methods.<sup>22</sup> Figure 6 shows the corresponding vibrational temperature profiles. The translational temperature profile has much higher value than the vibrational one, but the former relaxes much faster.

Probably this is the first time such a gaskinetic CFD scheme was developed, but we must point it out that the results in this paper are preliminary and the scheme is under further refinement.

## V. Conclusion

We have discussed some recent preliminary progress in developing a gaskinetic BGK CFD scheme to compute the inner structure of chemically reacting planar shock wave. We choose an example flow with two species, nitrogen gas and nitrogen atom, with chemical dissociation and combination reactions. The inner degrees of freedom are considered for the nitrogen gas, hence there are several temperatures in the equilibrium state to describe translational, rotational and vibrational energy. The nitrogen atom only has one temperature, and in this study we assume at the equilibrium upstream and downstream, nitrogen molecules and atoms have the same translational temperature and average velocity.

One key factor to successfully utilize this scheme for planar shock simulation is to accurately determine the downstream boundary conditions. Essentially this is a Dirichlet boundary problem instead of a Neumann boundary problem. We considered the balance of mass, momentum and energy between the upstream and downstream, both of them are assumed to be in equilibrium and all temperatures share the same equilibrium value, respectively.

A benchmark case was simulated with the gaskinetic CFD scheme. The comparison results show that this scheme is very promising to compute the inner structure of the shock waves with thermal nonequilibrium and chemical reactions. However, we must point it out that the problem itself is very complex, and the solution accuracy depends on levels of approximations. Hence, the work in this paper can only serve as an intermediate report, and some further investigations and refinement is currently in progress.

## Acknowledgments

Most work in this paper was completed while the first author worked for ZONA Technology Inc., it was partially supported by a STTR contract from U.S. Air Force Office of Scientific Research, via contract No.FA9550-06-C-0003 to ZONA Technology. The task was monitored by Dr. John Schmisser and Dr. Jonathan Poggie.

## References

- <sup>1</sup>Zel'dovich, Ya.B. and Raizer, Yu.P., Edited by Hayes, W.D. and Probstein, R.F., *Physics of Shock Waves and High-Temperature Hydrodynamic Phenomena*, Dover Publications, Mineola, 2002.
- <sup>2</sup>Groppi, M., Aoki, K., Spiga, G. and Tritsch, V., "Shock Structure Analysis in Chemically Reacting Gas Mixtures by a Relaxation-Time Kinetic Model," *Physics of Fluids*, 20(11), 117103, 2008.
- <sup>3</sup>Groppi, M., Spiga, G. and Takata, S., "The Steady Shock Problem in Reactive Gas Mixtures," *Bulletin of the Institute of Mathematics*, Vol.2, No.4, pp.935-956, 2007, Academia Sinica.
- <sup>4</sup>Groppi, M., and Spiga, G., "A Bhatnagar-Groos-Krook Type Approach for Chemically Reacting Gas Mixtures," *Physics of Fluids*, Vol.16, No.12, 2004, pp. 4273-4284.
- <sup>5</sup>Rossani, A., and Spiga, G., "A Note on the Kinetic Theory of Chemically Reacting Gases," *Physica A*, 272, (1999), pp. 563-573.
- <sup>6</sup>Xu, K., "A Gas-Kinetic BGK Scheme for the Navier-Stokes Equations and Its Connection with Artificial Dissipation and Godunov Method," *Journal of Computational Physics*, 171(2001), 289-335.
- <sup>7</sup>Xu, K. and Eswar, J., "Multiple Translational Temperature Model and Its Shock Structure Solution," *Physical Review E*, Vol.71, 056308, 2005.
- <sup>8</sup>Xu, K., "Nonequilibrium Bhatnagar-Groos-Krook Model for Nitrogen Shock Structure," *Physics of Fluids*, Vol.16, No.10, 2004.
- <sup>9</sup>Kogan, K. N., *Rarefied Gas Dynamics*, Plenum, New York, 1969.
- <sup>10</sup>Xu, K. and Li, Z., "Microchannel Flow in the Slip Regime: Gas-Kinetic BGK-Burnett Solutions," *Journal of Fluid Mechanics*, (2004), Vol. 513, pp. 87-110.
- <sup>11</sup>Bird, G.A., *Molecular Gas Dynamics and the Direct Simulation of Gas Flows*, Clarendon Press, Oxford, New York, 1994.
- <sup>12</sup>Cai, C., Liu, D., and Xu, K. "A One-Dimensional Multiple-Temperature Gas Kinetic BGK Scheme for Shock Wave Computation," *AIJA Journal*, Vol.46, No.5, May 2008, pp.1054.
- <sup>13</sup>Bird, G.A., "Direct Molecular Simulation of a Dissociating Diatomic Gas," *Journal of Computational Physics*, Vol.25, Issue 4, 1977, pp.353-365.
- <sup>14</sup>Vincenti, W.G. and Kruger, C.H., *Introduction to Physics Gas Dynamics*, Chapter 5, John Wiley and Sons Inc., 1965.
- <sup>15</sup>Chapman, S. and Cowling, T.G., *The Mathematical Theory of Non-Uniform Gases*, Cambridge at the University Press, 1960.
- <sup>16</sup>Xu, K., *Gas-Kinetic Schemes for Unsteady Compressible Flow Simulations*, von Karman Institute for Fluid Dynamics Lecture Series, 1998-03.
- <sup>17</sup>Lian, Y.S. and Xu, K., "A Gas-Kinetic Schemes for Multimaterial Flows and Its Application in Chemical Reactions," *Journal of Computational Physics*, Vol. 163, 2000, pp. 349-375.
- <sup>18</sup>Koller, W., "A Semi-Continuous Extended Kinetic Model for Bimolecular Chemical Reactions," *Journal of Physics, A*, 33(2000), 6081-6094.
- <sup>19</sup>Andries, P., Aoki, K., and Perthame, B., "A Consistent BGK-Type Model for Gas Mixtures," *Journal of Statistical Physics*, Vol.106, No.516, March 2002, pp. 993-1018.
- <sup>20</sup>Boyd, I.D., "Monte Carlo Analysis of Dissociation and Recombination behind Strong Shock Waves in Nitrogen," *Shock Waves*, 1991, 1:169-176.
- <sup>21</sup>Kewley D.J. and Hornung H.G., "Free-Piston Shock Tube Study of Nitrogen Dissociation," *Chemical Physical Letter*, Vol. 25, No.4, 1974, pp.531-536.
- <sup>22</sup>Boyd, I.D., "A Threshold Line Dissociation Model for the Direct Simulation Monte Carlo Method," *Physics of Fluids*, 8(5), May, 1996, pp.1293-1330.
- <sup>23</sup>Xu, K., "Regulation of the Chapman-Enskog Expansion and Its Description of Shock Structure," *Physics of Fluids*, Vol.14, Number 4, 2002.

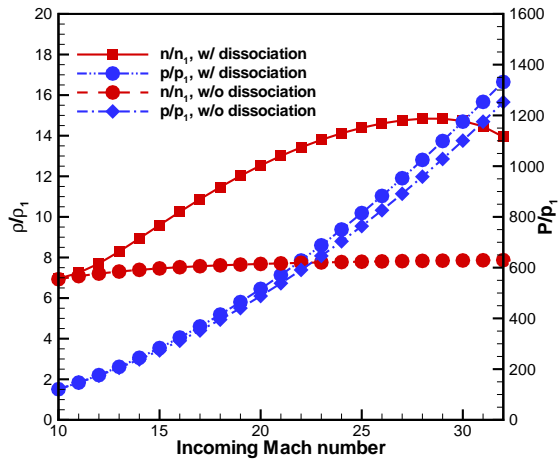


Figure 1. Post-shock equilibrium state pressure and number density profiles (free stream is nitrogen gas,  $\rho_\infty = 1.741315 \times 10^{-2} \text{ kg/m}^3$ ,  $T_\infty = 226.649 \text{ K}$ ).

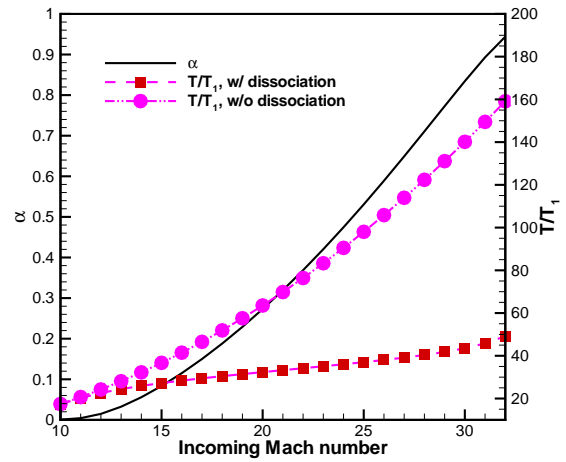


Figure 2. Post-shock equilibrium state temperature and dissociation degree profiles (free stream is nitrogen gas,  $\rho_\infty = 1.741315 \times 10^{-2} \text{ kg/m}^3$ ,  $T_\infty = 226.649 \text{ K}$ ).

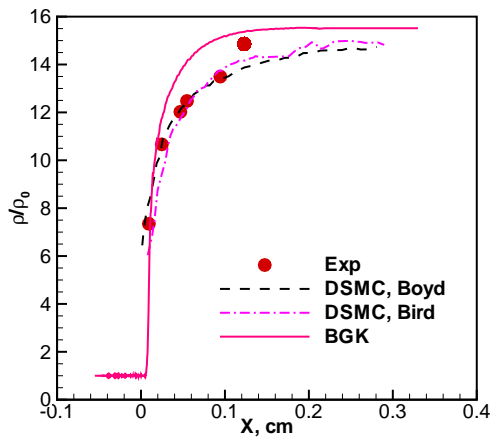


Figure 3. Comparison of normalized density profiles across a shock wave: experimental measurements, numerical results computed by DSMC and gaskinetic BGK methods ( $Z_{vib,BGK} = 30$ ,  $Z_{rot,BGK} = 3$ , free stream is nitrogen gas,  $p_\infty = 666.1 \text{ Pa}$ , density  $\rho_\infty = 7.48 \times 10^{-3} \text{ kg/m}^3$ ,  $U_\infty = 7310 \text{ m/s}$ ).

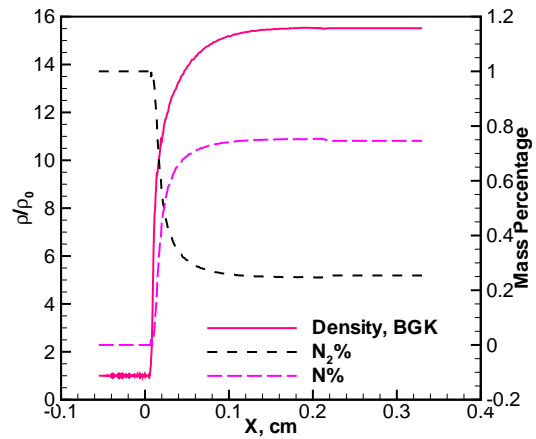


Figure 4. Profiles of density and mass percentage for  $N_2$  gas and nitrogen atom across the shock wave computed by the gaskinetic BGK method ( $Z_{vib,BGK} = 30$ ,  $Z_{rot,BGK} = 3$ , free stream is nitrogen gas,  $p_\infty = 666.1 \text{ Pa}$ , density  $\rho_\infty = 7.48 \times 10^{-3} \text{ kg/m}^3$ ,  $U_\infty = 7310 \text{ m/s}$ ).

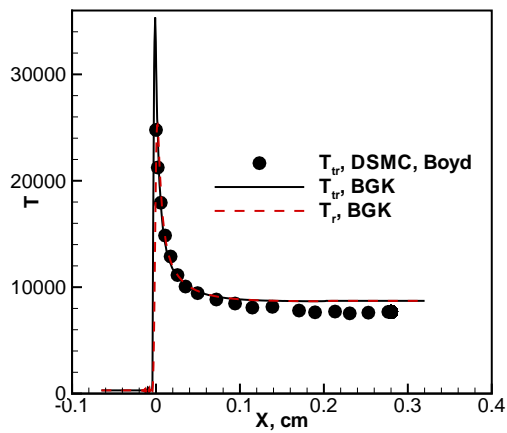


Figure 5. Translational temperature profiles computed by gaskinetic BGK and DSMC methods ( $Z_{vib,BGK} = 30, Z_{rot,BGK} = 3$ , free stream is nitrogen gas,  $p_1=666.1$  Pa, density  $\rho_\infty = 7.48 \times 10^{-3}$  kg/m<sup>-3</sup>,  $U_\infty = 7310$  m/s.)

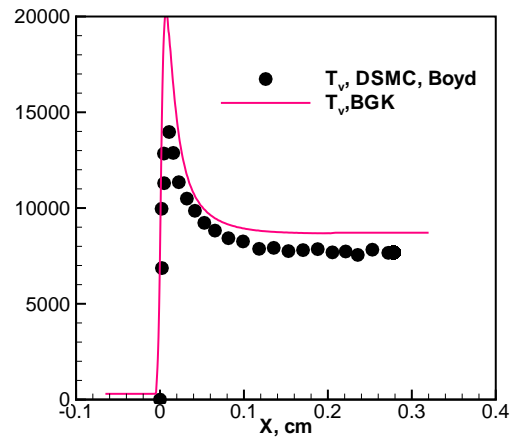


Figure 6. Vibrational temperature profiles computed by gaskinetic BGK and DSMC methods ( $Z_{vib,BGK} = 30, Z_{rot,BGK} = 3$ , free stream is nitrogen gas,  $p_1=666.1$  Pa, density  $\rho_\infty = 7.48 \times 10^{-3}$  kg/m<sup>-3</sup>,  $U_\infty = 7310$  m/s).